Micro-PIXE analysis on adsorbent of extraction chromatography for MA(III) recovery

Y. Takahatake, S. Watanabe, H. Kofuji, M. Takeuchi, K. Nomura
Japan Atomic Energy Agency, Tokai-mura, Naka-gun, Ibaraki 319-1194, Japan

T. Satoh
National Institutes for Quantum and Radiological Science and Technology
Takasaki, Gunma 370-1292, Japan

ABSTRACT

JAEA has been conducting research and development of MA(III) recovery from HLLW by extraction chromatography technology for reduction in amount and environmental impact of radioactive waste. The behavior of adsorbed cations inside the adsorbent packed in a column is necessary to be evaluated for improvement of the adsorbent or flow-sheet to achieve targeted MA(III) recovery performance. In this paper, micro-PIXE analysis was carried out on the particles sampled from various positions of the column to reveal the behavior of cations inside the packed column with CMPO/SiO_2-P adsorbent using RE(III) as simulated elements of MA(III). Simple experiment and data analysis were shown to be effective to reveal inside of the column, and formation and transportation of the adsorption bands were observed for some cations which are extractable by the CMPO extractant. Some part of Zr(IV) and Mo(VI) were found to remain inside the column without distinct transportation even after the elution operation. Those results will contribute to design more practical MA(III) recovery flow-sheet.

Keywords: micro-PIXE analysis, reprocessing, extraction chromatography, minor actinide, CMPO

1. Introduction

High level liquid waste (HLLW) generated in the reprocessing of spent nuclear fuel contains many kind of radioactive nuclides. The HLLW is planned to be vitrified and geologically disposed. Minor actinides (MA(III): Am(III) and Cm(III)) contained in the HLLW are known to be long-lived and/or heat-generating nuclides, and those are desirable to be removed in order to reduce potential hazard of the vitrified radioactive waste. Japan Atomic Energy Agency (JAEA) has been conducting research and development of the extraction chromatography technology for establishing MA(III) recovery process [1,2]. In this technology, MA(III) is recovered from the HLLW through adsorption/elution reactions between the cations with adsorbent packed in a column. The adsorbent is prepared by impregnating an extractant into SiO_2-P which is porous silica particles coated by styrene-divinylbenzene co-polymer[3]. Fig. 1 shows a representative scheme of MA(III) recovery flow diagram by the extraction chromatography. MA(III) and rare earth elements (RE(III)) are recovered by the 1st column, and then MA(III) are separated from RE(III) by the 2nd column. In our current flow-sheet, octyl(phenyl)-N,N-diisobutylcarbamoylmethylphosphine oxide (CMPO) [4] and bis(2-ethylhexyl) hydrogen phosphate (HDEHP) [5] extractants are utilized in the adsorbent for the 1st and 2nd columns, respectively.

The previous column separation experiment showed that some improvements on the flow-sheet or structure of the adsorbents might be required to achieve our targeted MA(III) recovery ratio and decontamination factors of fission products [6]. Experiments using MA(III) are essential for developments in the adsorbents or in the flow-sheet, however possible operations and analyses are limited due to their strong radioactivity. Therefore, fundamental characterization and screening are generally conducted under inactive environment with using simulated elements. Improvements of SiO_2-P adsorbent with trial and error process require much time and frequent experiments, thus more efficient procedure is required to be developed. Simultaneous visualizations of cations inside the small silica particles and in the column during the operation would significantly contribute to identify the points to be improved. In our previous studies, micro-PIXE and X-ray absorption analyses were revealed to be powerful tools for investigating distributions of adsorbed cations inside the particle and the column, respectively [7-9]. Although combination of those two experimental techniques is effective, those analyses have to be carried out in different facilities with limited available time. Single experiment and simple data analysis are required for the practical use in evaluation of the extraction chromatography adsorbent and process. In this study, the behavior of cations inside the CMPO/SiO_2-P particle during the column operation was tried to be investigated only by micro-PIXE analysis to establish simple evaluation method for the extraction chromatography process.

MA(III): Minor actinides (Am(III) and Cm(III))
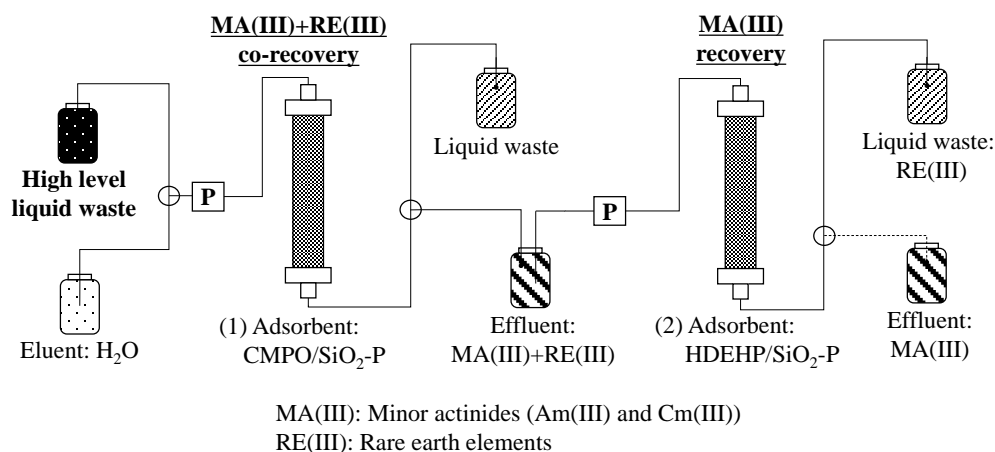RE(III): Rare earth elements

Fig. 1.   A representative scheme of MA(III) recovery flow diagram and the adsorbents utilizing our current flow-sheet.

2.   Materials and Methods

Average diameter and pore size of SiO_2-P used in this study were 50 µm and 50 nm, respectively. Impregnation of CMPO (Fig. 2) into SiO_2-P was carried out according to the article [3].   CMPO/SiO_2-P was packed in the glass column of 1 cmID and 32.5 cmH.   After supplying excess amount of simulated HLLW against adsorption capacity of the column, deionized water was supplied as an eluent.   The effluent was fractionally collected at every 1 bed volume (BV; 25.5 cm³).   Concentrations of cations in the feed solution and the fractions were determined by ICP-AES analysis.   Composition of the simulated HLLW is shown in Table 1, where Eu(III) is simulated element for MA(III).   After the adsorption operation or the adsorption/elution operation, the CMPO/SiO_2-P were sampled at every 5 cm from the top of the column, and then dried at 60 °C in atmospheric environment. Those particles were supplied to the micro-PIXE analysis.

The micro-PIXE analysis was held on the single-ended accelerator at Takasaki Advanced Radiation Research Institute.   Proton beams accelerated up to 3 MeV were transported to a microbeam formation system.   The beams were focused to a spot approximately 1×1 µm² on particles of CMPO/SiO_2-P.   Average beam current was 100 pA, and the scanning size was set at 100×100 µm².   Characteristic X-rays from the target were detected by a Si(Li) detector with a 100-µm-thick fanny filter having a 3-mm diameter pinhole for preventing recoiled protons.

Extended X-ray Absorption spectra of some sample particles were collected at BL27B beamline of Photon Factory of High Energy Accelerator Research Organization (KEK), Japan, to support a discussion.
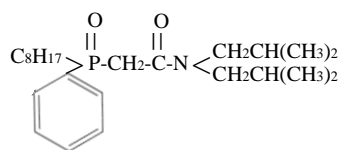

Fig. 2.   Chemical structure of CMPO.

Table 1.   Composition of the feed solution through the column that simulated HLLW. The solution was prepared by non-radioactive nuclides.

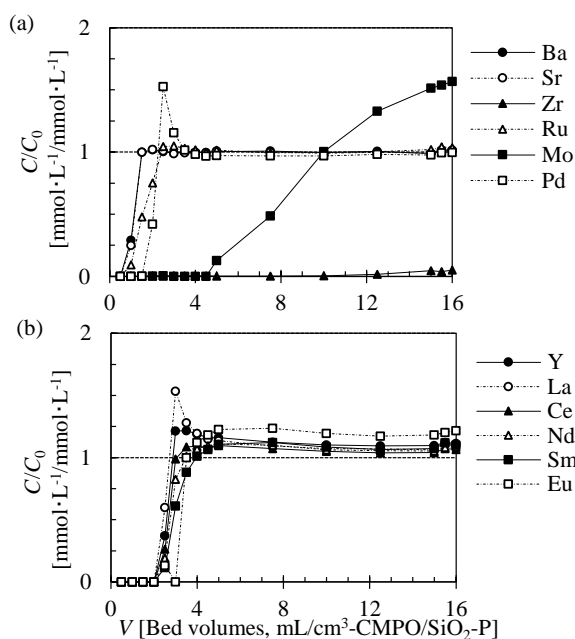| Component	Ba	Sr	Zr	Ru	Y	La	Ce	Nd	Sm	Eu	Mo	Pd	H+
Concentration [mmol/L]	7.8	7.3	17	14	3.5	6.4	48	21	4.7	0.64	9.2	7.0	4000

Fig. 3. Breakthrough curves of cations in the simulated HLLW for the CMPO/SiO₂-P packed column. Results are separately shown in two figures (a) and (b) for easy to being understood. (a) Ba, Sr, Zr, Ru, Mo and Pd. (b) Y, La, Ce, Nd, Sm and Eu. C_0 is concentration of the cations in the feed solution, C is concentration of that in a fraction of effluent. V is flow volume of solutions. After the operation, CMPO/SiO₂-P were sampled at every 5 cm from the top of the column.

Fig. 4. X-ray spectra of CMPO/SiO₂-P particle after the adsorption operation obtained by micro-PIXE analysis. CMPO/SiO₂-P particles were sampled after the operation shown in Fig. 3. (a) Upper part of the column (0- 5 cm from the top). (b) Middle part (15- 20 cm). (c) Bottom part (30-32.5 cm).

3. Results and discussion

Breakthrough curves of cations in the simulated HLLW for the CMPO/SiO₂-P packed column are shown in Fig. 3, here C and C_0 correspond to concentrations of cations in the effluent and the feed solution, respectively. When C/C_0 increased up to 1, adsorption of the CMPO/SiO₂-P column reached at equilibrium. The value of C/C_0 above 1 must be elution of elements from CMPO/SiO₂-P as a result of competitive adsorption of cations. Ba(II), Sr(II) and Ru(III) were not adsorbed by CMPO/SiO₂-P, and these results reasonably agree with the previous report [2]. RE(III)−Y(III), La(III), Ce(III), Nd(III), Sm(III) and Eu(III)− were adsorbed by the column, and they showed breakthrough at $V = 2$ BV, where breakthrough of this paper means 5 % breakthrough. While larger amount of Zr(IV) and Mo(VI) were adsorbed than RE(III), and they finally show their breakthrough at $V = 4$ and 15 for Mo(VI) and Zr(IV), respectively. The adsorbed RE(III) were gradually discharged from the column with progress in adsorption of Zr(IV) and Mo(VI). These results suggest that Zr(IV) and Mo(VI) are preferentially adsorbed by the CMPO/SiO₂-P. As MA(III) behave like RE(III) in the CMPO/SiO₂-P column, concentrations of Zr(IV) and Mo(VI) in the HLLW would significantly influence on throughput and performance of the MA(III) recovery process. More detail transportation behavior of RE(III), Zr(IV) and Mo(VI) in the column are necessary to be comprehended in order to design an optimized flow-sheet with the largest throughput and efficiency.

Characteristic X-ray spectra of the CMPO/SiO₂-P particle sampled from the column at $Z = 0$-5 (upper part), 15-20 (middle part) and 30-32.5 (bottom part) cm after the adsorption operation are shown in Fig. 4. Peaks of Si and P were originated from porous silica particle and CMPO, respectively, and those of other elements were attributed to the adsorbed elements. Amount of RE(III) are seemed to increase with coming down from the inlet to the outlet of the column, which must be reasonably explained by transportation of RE(III) caused by occupation of the adsorption sites with Zr(IV) and Mo(VI).

Table 2 shows density of RE(III) in the CMPO/SiO₂-P calculated by X-ray absorption spectra of the sampled adsorbent from middle part of the column with the mass absorption coefficients of the corresponding elements [10].
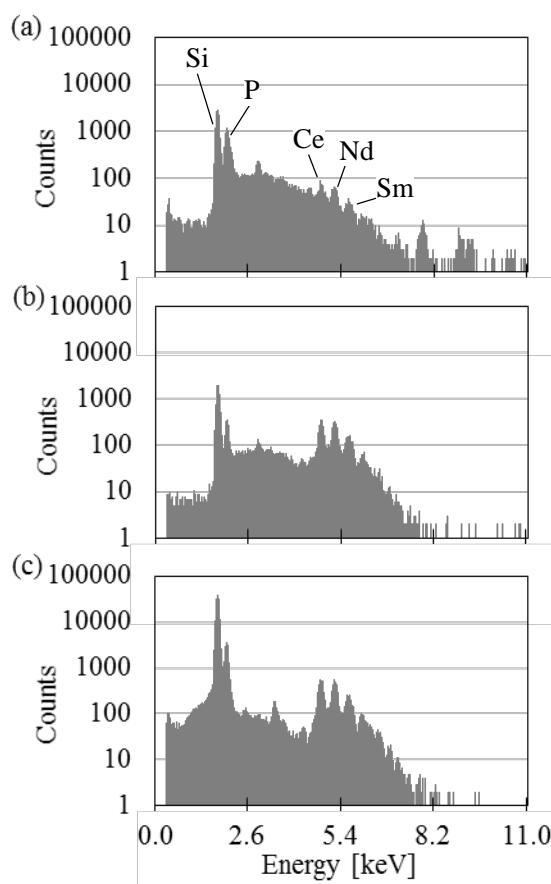
Table 2. Density of elements in the CMPO/SiO$_2$-P at middle part of the column after the adsorption operation.

Element	Density of element [g/cm^3]
Y	3.2×10^{-4}
La	2.1×10^{-4}
Ce	4.7×10^{-3}
Nd	5.1×10^{-3}
Sm	2.3×10^{-3}
Eu	1.7×10^{-4}
Pr	4.6×10^{-4}

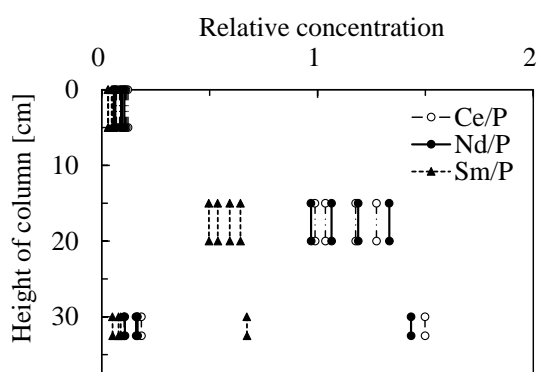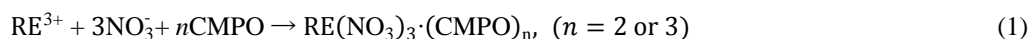

Fig. 5. Variation of relative concentration of Ce, Nd and Sm to P with height of the column after the adsorption operation.

Fig. 6. X-ray spectra of the CMPO/SiO$_2$-P particle after the adsorption/elution operation obtained by micro-PIXE analysis. (a) Upper part of the column (0- 5 cm from the top). (b) Middle part (15- 20 cm). (c) Bottom part (30-32.5 cm).

Seven RE(III) were found in CMPO/SiO$_2$-P where Pr(III) might be impurities in regents of other RE(III), and three high density elements−Ce(III), Nd(III) and Sm(III)− were identified in spectra obtained by micro-PIXE analysis, shown in Fig. 4.

Peak intensities of Ce(III), Nd(III) and Sm(III) in a spectrum cannot be directly compared with those in other spectra due to differences in 1) the dose rate for the analysis, 2) shape and size of the particles and 3) the concentration of the CMPO extractant in the particles. Normalization of intensities of peaks for Ce(III), Nd(III) and Sm(III) is necessary for the comparison. RE(III) form complex with CMPO according to the equation (1), and the normalization can be achieved by dividing intensities of Ce(III), Nd(III) and Sm(III) by that of P (referred to "Ratios of peak intensities").

$$RE^{3+} + 3NO_3^- + n\text{CMPO} \rightarrow RE(NO_3)_3 \cdot (\text{CMPO})_n, \quad (n = 2 \text{ or } 3) \tag{1}$$

Those data gives information of relative concentrations of adsorbing RE(III) on the particle normalized with concentration of CMPO, and influence of such as particle shape and size on the concentrations should be canceled. Ratios of peak intensities of Ce(III), Nd(III) and Sm(III) to that of P are shown in Fig. 5. Four or five particles on each part were analyzed, and the results about all analyzed particles are shown. Most relative concentration profiles showed the maximum of the ratios of peak intensities at 15-20 cm, and the maximum is considered to be the adsorption bands of RE(III). On one particle at the bottom part of the column, three relative concentrations showed high value, and which reasonably agree with the elution of RE(III) resulted from the competitive adsorption of cations. Consequently, we could conclude that simple data treatment of the micro-PIXE analysis on the adsorbent sampled from the column has potential to reveal the transport of cations inside the packed column.

Fig. 6 shows the characteristic X-ray spectra of particles sampled after the adsorption/elution operation. The peaks of Ce(III), Nd(III) and Sm(III) were not observed. So Ce(III), Nd(III) and Sm(III) were discharged by the elution operation.
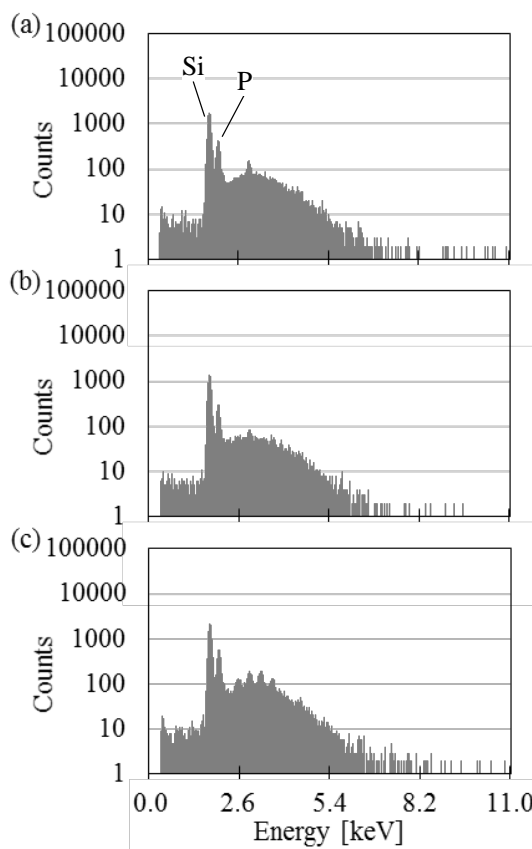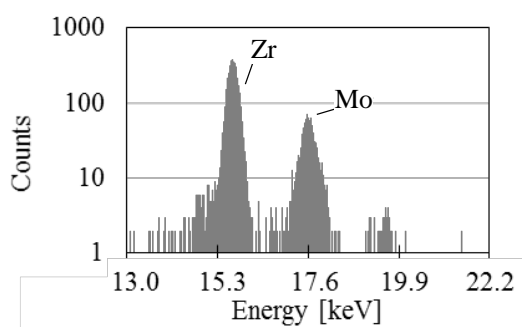
Fig. 7. X-ray spectrum of the CMPO/SiO₂-P particle sampled at upper part of the column (0- 5 cm from the top) after the adsorption operation obtained by micro-PIXE analysis. The particle was same as that showed analysis result in Fig. 4 (a).
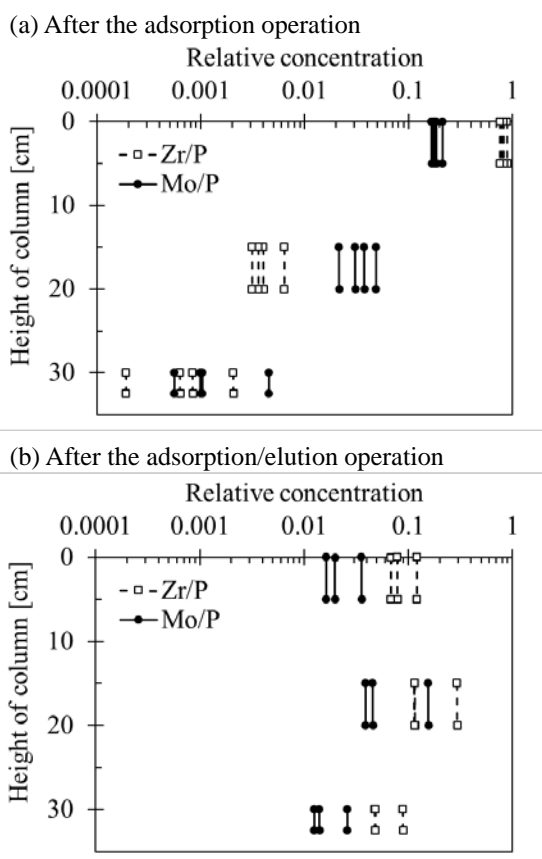
(a) After the adsorption operation

(b) After the adsorption/elution operation

Fig. 8. Ratios of peak intensities of Zr(IV) and Mo(VI) to P on the CMPO/SiO₂-P particles with height of column. (a) After the adsorption operation, (b) After the adsorption/elution operation. Relative concentration of Zr/P and Mo/P on original particles are under about 0.001.

Fig. 7 shows X-ray spectrum obtained by the PIXE analysis on the CMPO/SiO₂-P particle sampled from upper part of the column after the adsorption operation, here the characteristic lines of Zr(IV) and Mo(VI) were observed. Breakthrough curves shown in Fig. 3 suggest that Zr(IV) and Mo(VI) were preferentially adsorbed by the CMPO/SiO₂-P, and this feature agrees with the X-ray profile.

Ratios of peak intensities of Zr(IV) and Mo(VI) to that of P are shown in Fig. 8. Just after the adsorption operation, those took the maximums at upper part of the column and adsorption of Zr(IV) and Mo(VI) at bottom part were almost negligible. Mo/P was larger than Zr/P at middle part, thus some part of Mo(VI) must be transferred to downward as a result of adsorption competition with Zr(IV) regarding the breakthrough behavior of them. Even after supplying the eluent into the column, both Zr(IV) and Mo(VI) remained inside the column though their adsorption bands seemed to move to downstream of the column. Zr(IV) and Mo(VI) are selectively extracted by CMPO and hardly eluted by water, and this characteristics can reasonably explain the previous experimental data[2]. The adsorbed Zr(IV) and Mo(VI) have to be washed out by an appropriate wash solution before the end of operation, because the remaining Zr(IV) and Mo(VI) in CMPO/SiO₂-P suppress adsorption of MA(III) as well as RE(III) in case of reuse of the column. X-ray absorption of the particle surely showed the existence of Zr, and EXAFS analysis on the spectrum with WinXAS 2.3 [11] and FEFF8.0 [12] suggests that Zr(OH)₄ forms complex with CMPO inside the particle. Back-extraction of Zr(OH)₄ from the complex with CMPO has to be established for the practical use of the technology. Decontamination of Zr(IV) and Mo(VI) in advance with MA(III) recovery process is also effective. Our previous experiments showed that HDEHP/SiO₂-P is applicable to selectively removing Zr(IV) and Mo(VI) from acidic solution, although elution of Zr(IV) from the adsorbent is still difficult[13]. An appropriate procedure or process will be employed in the near future based on fundamental studies.

4.   Conclusion

The behavior of cations inside the CMPO/SiO₂-P particle during the column operation were discussed only by micro-PIXE analysis for simple evaluation of the extraction chromatography process. The adsorption bands of RE(III) which behaves like MA(III) were suggested by considering about relative concentrations. Some part of Zr(IV) and Mo(VI) was found to remain inside the column without distinct transportation even after the elution operation. So, back-extraction operation of the specie has to be considered for the practical use of MA(III) recovery process, and decontamination of Zr(IV) and Mo(VI) in advance with MA(III) recovery process is also effective when reusing the column.   Simple experiment and data analysis of micro-PIXE were shown to be effective to reveal inside the column, and those results will contribute to design more practical MA(III) recovery flow-sheet.

References
1. S. Watanabe, I. Goto, K. Nomura, Y. Sano, Y. Koma, Extraction Chromatography Experiments on Repeated Operation Using Engineering Scale Column System, Energy Procedia, 7, 449-453 (2011).
2. S. Watanabe, T. Senzaki, A. Shibata, K. Nomura, Y. Koma, Y. Nakajima, MA recovery experiments from genuine HLLW by extraction chromatography, Proceedings of Global 2011, Makuhari, Japan, December 11-16, 2011, Paper 387433, CD-ROM (2011)
3. Y.-Z. Wei, K.N. Sabharwal, M. Kumagai, T. Asakura, G. Uchiyama, S. Fujine, Studies on the separation of minor actinides from high-level wastes by extraction chromatography using novel silica-based extraction resins, Nucl. Technol. 132, 3, 413-423 (2000)
4. E. P. Horwitz, D. G. Kalina, H. Diamond, G. F. Vandegrift, W. W. Schulz, The TRUEX Process - A Process for the Extraction of the Transuranic Elements from Nitric Acid Wastes Utilizing Modified PUREX Solvent, Solvent Extraction and Ion Exchange, 3(1&2), 75-109 (1985)
5. B. Weaver, F. A. Kappelmann, TALSPEAK: A New Method of Separating Americium and Curium from the Lanthanides by Extraction from an Aqueous Solution of an Aminopolyacetic Acid Complex with a Monoacidic Organophosphate or Phosphonate, ORNL-3559 (1964)
6. S. Watanabe, K. Nomura, S. Kitawaki, A. Shibata, H. Kofuji, Y. Sano, M. Takeuchi, Flow-sheet study of MA recovery by extraction chromatography for SmART cycle project, Procedia Chemistry, 21, 101-108 (2016)
7. T. Satoh, A. Yokoyama, A. Kitamura, T. Ohkubo, Y. Ishii, Y. Takahatake, S. Watanabe, Y. Koma, W. Kada, Particle induced X-ray emission-computed tomography analysis of an adsorbent for extraction chromatography, Nuclear Instruments and Methods in Physics Research B 371, 419-423 (2016)
8. S. Watanabe, Y. Sano, M. Myouchin, Y. Okamoto, H. Shiwaku, A. Ikeda-Ohno, S. Suzuki, T. Yaita, In-Situ Analysis of Chemical State and Ionic Distribution in the Extraction Chromatography Column, J. Ion Exchange, 21, 3, 189-194 (2010)
9. S. Watanabe, Y. Sano, H. Shiwaku, T. Yaita, S. Ohno, T. Arai, H. Matsuura, M. Koka, T. Satoh, Local structure and distribution of remaining elements inside extraction chromatography adsorbents, Nuclear Instruments and Methods in Physics Research B (in press)
10. J. H. Hubbell, S. M. Seltzer, Table of X-Ray Mass Attenuation Coefficients and Mass Energy-Absorption Coefficients from 1 keV to 20 MeV for Elements Z = 1 to 92 and 48 Additional Substances of Dosimetric Interest, https://www.nist.gov/pml/x-ray-mass-attenuation-coefficients, NIST PHYSICAL MEASUREMNT LBORATORY, NIST Standard Reference Database 126, May 1996 Release
11. T.Ressler, WinXAS; a Program for X-ray Absorption Spectroscopy Data Analysis under MS-Windows, J. Synchrotron Rad. 5, 118-122 (1998)
12. S. I. Zabinsky, J. J. Rehr, A. Aukudinov, R. C. Albers, M. J. Eller, FEFF8.0; Multiple-scattering calculations of X-ray-absorption spectra, Phys. Rev. B52, 2995 (1995)
13. R. Abe, K. Nagoshi, T. Arai, S. Watanabe, Y. Sano, H. Matsuura, H. Takagi, N. Shimizu, M. Koka, T. Satoh, Microscopic analyses of complexes fromed in adsorbent for Mo and Zr separation chromatography, Nuclear Instruments and Methods in Physics Research B (in press)